nature biomedical engineering

ARTICLES

https://doi.org/10.1038/s41551-020-0546-5

Check for updates

A CRISPR-based assay for the detection of opportunistic infections post-transplantation and for the monitoring of transplant rejection

Michael M. Kaminski[1,2,3], Miguel A. Alcantar[1], Isadora T. Lape[4], Robert Greensmith[2,3], Allison C. Huske[1], Jacqueline A. Valeri[1,5], Francisco M. Marty[6], Verena Klämbt[7], Jamil Azzi[4], Enver Akalin[8], Leonardo V. Riella[4] ✉ and James J. Collins[1,5,9] ✉

In organ transplantation, infection and rejection are major causes of graft loss. They are linked by the net state of immunosuppression. To diagnose and treat these conditions earlier, and to improve long-term patient outcomes, refined strategies for the monitoring of patients after graft transplantation are needed. Here, we show that a fast and inexpensive assay based on CRISPR–Cas13 accurately detects BK polyomavirus DNA and cytomegalovirus DNA from patient-derived blood and urine samples, as well as *CXCL9* messenger RNA (a marker of graft rejection) at elevated levels in urine samples from patients experiencing acute kidney transplant rejection. The assay, which we adapted for lateral-flow readout, enables—via simple visualization—the post-transplantation monitoring of common opportunistic viral infections and of graft rejection, and should facilitate point-of-care post-transplantation monitoring.

The CRISPR and Cas immune system has recently been adapted for the detection of nucleic acids[1–8]. These protocols enable rapid, cost-effective DNA and RNA detection in a variety of sample types with excellent sensitivity and specificity, making them ideal tools for point-of-care (POC) testing. However, most studies to date have used synthetic standards, include few clinical specimens, and lack direct comparison to clinical gold-standard diagnostics. Here, we applied and optimized the CRISPR–Cas13 specific high-sensitivity enzymatic reporter unlocking (SHERLOCK) technology for diagnosis of biomarkers highly relevant for renal-transplant recipients.

Since the first successful kidney transplantation in 1954, substantial improvements in short-term outcomes have been achieved in organ transplantation. However, there has been less progress in long-term outcomes, with more than half of the transplanted organs being lost after 10 yr[9,10]. Opportunistic infections and transplant-organ rejection are leading causes of graft loss, requiring careful adjustment of immunosuppression and life-long monitoring of post-transplant patients[11].

Current diagnostics, however, involve the use of expensive laboratory equipment and intricate multistep protocols, leading to limited availability, high costs and slow turnaround time[12,13]. Diagnosis of infections using PCR can take several days in clinical settings, and rejection diagnostics require invasive biopsies and histopathological analysis. These factors result in delays in pertinent diagnoses and increase the risk of irreversible allograft injury, especially in resource-limited settings. POC or at-home testing could greatly reduce associated costs and enable more frequent monitoring, which would lead to earlier diagnosis and treatment of graft dysfunction and common infections.

In this study, we developed CRISPR-based diagnostic tools for cytomegalovirus (CMV) and BK polyomavirus (BKV) infection, two common opportunistic viruses that are highly relevant for renal-transplant patients[14] and other immunocompromised patients[15,16]. Testing of more than 100 clinical specimens from patients infected with BKV and CMV over a wide range of virus loads revealed high diagnostic accuracy. We further extended the capability of SHERLOCK to the detection of human *CXCL9* mRNA, a biomarker indicative of rejection in renal-transplant recipients[17–19]. We anticipate that CRISPR–Cas13-based technologies will be broadly applicable for personalized medicine diagnostics, where repeated testing of biomarkers indicative of disease activity is key to early and effective secondary prevention.

Results

Optimization of the CRISPR–Cas13 SHERLOCK technology for the detection of BKV and CMV virus from patient samples. To test for active BKV and CMV infection, we isolated DNA from blood and urine of both infected patients and uninfected control patients (Fig. 1a). Subsequently, we applied a modified version of the SHERLOCK protocol for BKV and CMV detection. In brief, conserved regions of BKV and CMV were amplified using isothermal recombinase polymerase amplification (RPA). Incorporation of the T7 promoter sequence into forward primers enabled subsequent

[1]Institute for Medical Engineering and Science and Department of Biological Engineering, Massachusetts Institute of Technology, Cambridge, MA, USA. [2]Berlin Institute for Medical Systems Biology, Max Delbrück Center for Molecular Medicine in the Helmholtz Association, Berlin, Germany. [3]Department of Nephrology and Medical Intensive Care, Charité–Universitätsmedizin Berlin, Berlin, Germany. [4]Schuster Transplantation Research Center, Brigham and Women's Hospital, Harvard Medical School, Boston, MA, USA. [5]Wyss Institute for Biologically Inspired Engineering, Harvard University, Boston, MA, USA. [6]Division of Infectious Diseases, Brigham and Women's Hospital, Boston, MA, USA. [7]Department of Medicine, Boston Children's Hospital, Harvard Medical School, Boston, MA, USA. [8]Montefiore Einstein Center for Transplantation, Montefiore Medical Center, Albert Einstein College of Medicine, Bronx, NY, USA. [9]Infectious Disease and Microbiome Program, Broad Institute of MIT and Harvard, Cambridge, MA, USA. ✉e-mail: lriella@bwh.harvard.edu; jimjc@mit.edu

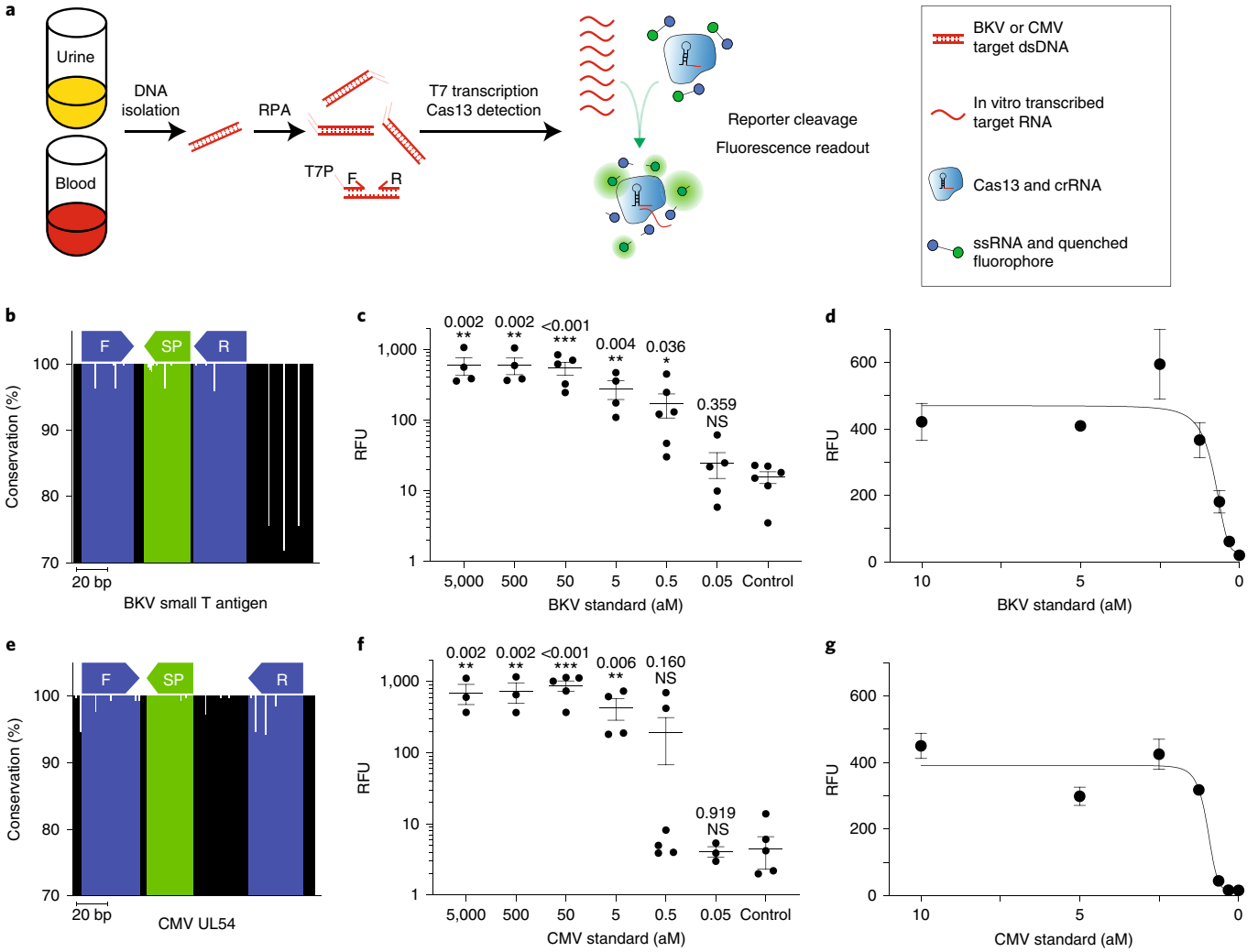

Fig. 1 | CRISPR diagnostics enable single-molecule detection of BKV and CMV DNA. a, Schematic illustrating the assay. After isolation of DNA from urine or blood, CMV and BKV target regions are amplified by RPA. T7 transcription of the RPA products allows for Cas13 detection of target RNA and subsequent collateral cleavage of reporter molecules. T7P, T7 promoter; F, RPA forward primer; R, RPA reverse primer; dsDNA, double-stranded DNA. **b**, BKV target-region conservation among all BKV strains. SP, crRNA spacer. **c**, CRISPR-based detection of the BKV synthetic standard at indicated concentrations. Data are mean ± s.e.m., $n \geq 4$ independent experiments. RFU, relative fluorescence units. **d**, CRISPR-based detection of the BKV synthetic standard in the attomolar range. Data are mean ± s.d. of three independent reactions. **e**, CMV target region conservation among all CMV strains. **f**, CRISPR-based detection of the CMV standard. Data are mean ± s.e.m., $n \geq 3$ independent experiments. **g**, CRISPR-based detection of the CMV synthetic standard in the attomolar range. Data are mean ± s.d. of three independent reactions. Difference from control assessed by two-tailed Student's *t*-test; NS, not significant; $^{*}P < 0.05$, $^{**}P < 0.01$, $^{***}P < 0.001$ and $^{****}P < 0.0001$ (**c**,**f**).

in-vitro RNA transcription using T7 polymerase. A CRISPR guide RNA (crRNA) complementary to 28 nucleotides of the RPA product was used to direct Cas13 from *Leptotrichia wadei* (LwaCas13a) to the target sequence. Detection of the target resulted in Cas13 activation and subsequent collateral cleavage of an oligonucleotide carrying a quenched fluorophore that exhibits fluorescence when cleaved, correlating with the initial concentration of the target in the patient sample[1].

To identify conserved regions in the BKV genome, we aligned all strains accessible from the National Center for Biotechnology Information (NCBI) and focused on target regions with sequence homology of more than 95% among all strains (Fig. 1b). Next, we tested 12 different primer pairs and 3 crRNAs for their ability to detect the BKV genes *STA*, *VP2* and *VP3* (Supplementary Fig. 1a). We identified a crRNA–primer pair specific for the small T antigen (STA), which allowed detection of the American Type Culture Collection (ATCC) quantitative synthetic BKV standard (Dunlop strain) down to the low attomolar range (0.3 aM), representing single-molecule detection in the assay volumes used (Fig. 1c,d). Notably, systematic assessment of various forward and reverse primer concentrations (Supplementary Fig. 1b) revealed that forward and reverse RPA primer concentrations of 120 nM and 480 nM, respectively, resulted in the highest sensitivity. Using a similar strategy, we identified a conserved region in the CMV UL54 gene (Fig. 1e) as a potential SHERLOCK target that enabled detection of the ATCC diagnostic CMV standard (strain AD-169) down to the low attomolar range (0.6 aM) (Fig. 1f,g).

Next, we tested whether the diagnostic performance of the SHERLOCK assay would be sufficient to detect BKV and CMV virus in urine and plasma samples from patients. Testing of 31 urine and 36 plasma samples showed that the optimized SHERLOCK

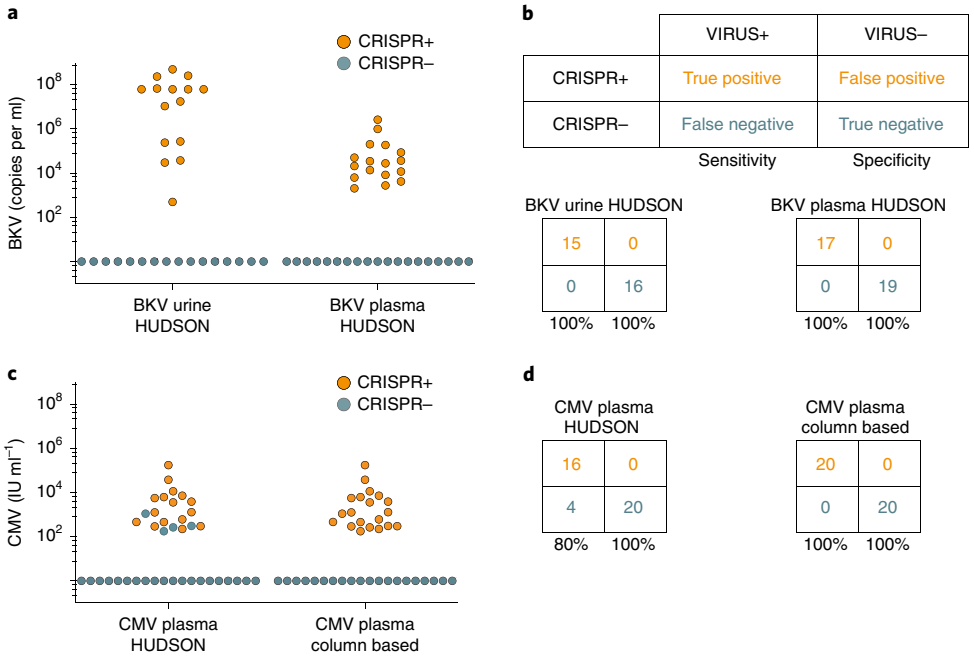

Fig. 2 | CRISPR detects BKV and CMV from human urine and blood samples over a wide range of viral loads. a, Testing for BKV virus in human urine ($n=31$) and plasma ($n=36$) samples, processed with HUDSON. Orange, CRISPR positive; blue, CRISPR negative. Virus copy numbers were assessed by qPCR and expressed as DNA copies per ml. **b**, Confusion matrix of samples tested in **a**. **c**, Testing for CMV virus from plasma samples as in **a** ($n=40$), isolated either with HUDSON or a commercial column-based kit. Virus copy-numbers were assessed by qPCR. **d**, Confusion matrix of samples tested in **c**.

protocol correctly identified all BKV specimens with 100% sensitivity and specificity (Fig. 2a,b and Supplementary Fig. 2a). Of note, this performance could be achieved using the rapid and simple heating unextracted diagnostic samples to obliterate nucleases (HUDSON) protocol[2], which involves heating of the sample for 10 min at 95 °C in the presence of tris(2-carboxyethyl)phosphine and EDTA, circumventing the need for time-consuming, column-based sample preparations (Supplementary Fig. 2b,c).

Similarly, the CRISPR assay enabled the detection of CMV-positive plasma samples with high sensitivity and specificity (Fig. 2c,d and Supplementary Fig. 2b,c). In contrast to our results with BKV, this performance could only be achieved using a commercial column-based viral DNA isolation kit; the HUDSON protocol resulted in lower sensitivity for low-copy-number samples (<1500 IU ml^{-1}). This difference in sensitivity is probably due to a sample concentration step included in the column-based kit.

CRISPR-based detection of *CXCL9* mRNA as a biomarker of kidney graft rejection. Next, we tested whether SHERLOCK could be applied to detect mRNA biomarkers indicative of kidney graft rejection. We selected *CXCL9* mRNA as a marker of rejection on the basis of its validation in multicentre studies[17,18,20].

For detection of *CXCL9* mRNA, we isolated RNA from pelleted urine cells (Fig. 3a). For amplification, we included a reverse transcriptase into the RPA reaction (RT–RPA). Using a synthetic RNA standard, Cas13 alone was sufficient to detect *CXCL9* in the low picomolar range, similar to the previously reported sensitivity (Fig. 3b). Addition of an RT–RPA reaction followed by T7 transcription and Cas13 activation enabled *CXCL9* detection in the attomolar range (Fig. 3b).

We next assessed whether this sensitivity was sufficient to discriminate patients undergoing kidney graft rejection ($n=14$) from a control group ($n=17$) (Supplementary Table 1). Rejection status was determined by gold-standard kidney biopsy (Supplementary Table 2).

We observed higher *CXCL9* mRNA levels in samples from patients with biopsy-proven rejection compared with transplant recipients with no rejection or stable graft function, which enabled us to detect kidney rejection with a sensitivity of 93% (Fig. 3c,d). The area under the receiver-operating-characteristic (ROC) curve was 0.91 (Fig. 3e).

We confirmed *CXCL9* mRNA upregulation in rejection samples with the quantitative PCR (qPCR) gold-standard assay[18], observing higher diagnostic accuracy compared with the CRISPR-based assay (Supplementary Fig. 3a–c). Detection of CXCL9 protein with an enzyme-linked immunosorbent assay (ELISA) showed lower sensitivity but higher specificity (Supplementary Fig. 3d–f) compared with CRISPR-based mRNA detection.

Rapid DNA isolation, CRISPR diagnostics and smartphone-based lateral-flow evaluation enable POC-ready detection of BKV and CMV infection. POC testing holds great promise for transplantation medicine, since fast and low-cost diagnostics could enable earlier treatment decisions and broader accessibility, thereby lowering the risk of irreversible transplant injury. To optimize BKV and CMV detection for POC testing, we combined the rapid HUDSON DNA-isolation protocol with SHERLOCK-based target detection and commercially available lateral-flow dipsticks (Fig. 4a). This method enabled an easy-to-read visual output that indicated a positive or negative test result. Since we observed that background noise can result in a faint test band on the lateral-flow strip, we developed a smartphone-based software application that allowed quantification of band intensities (Supplementary video 1). Here, the software calculates the ratio of test to control band intensities using images taken with a smartphone camera, enabling simple and rapid discrimination between negative and positive test results. The total turnaround time from isolation to sample detection was below 2 h.

We next tested the lateral-flow readout for the detection of the CMV and BKV synthetic standard (Fig. 4b,c). Similar to our fluorescence-based readout, we could detect both targets down to

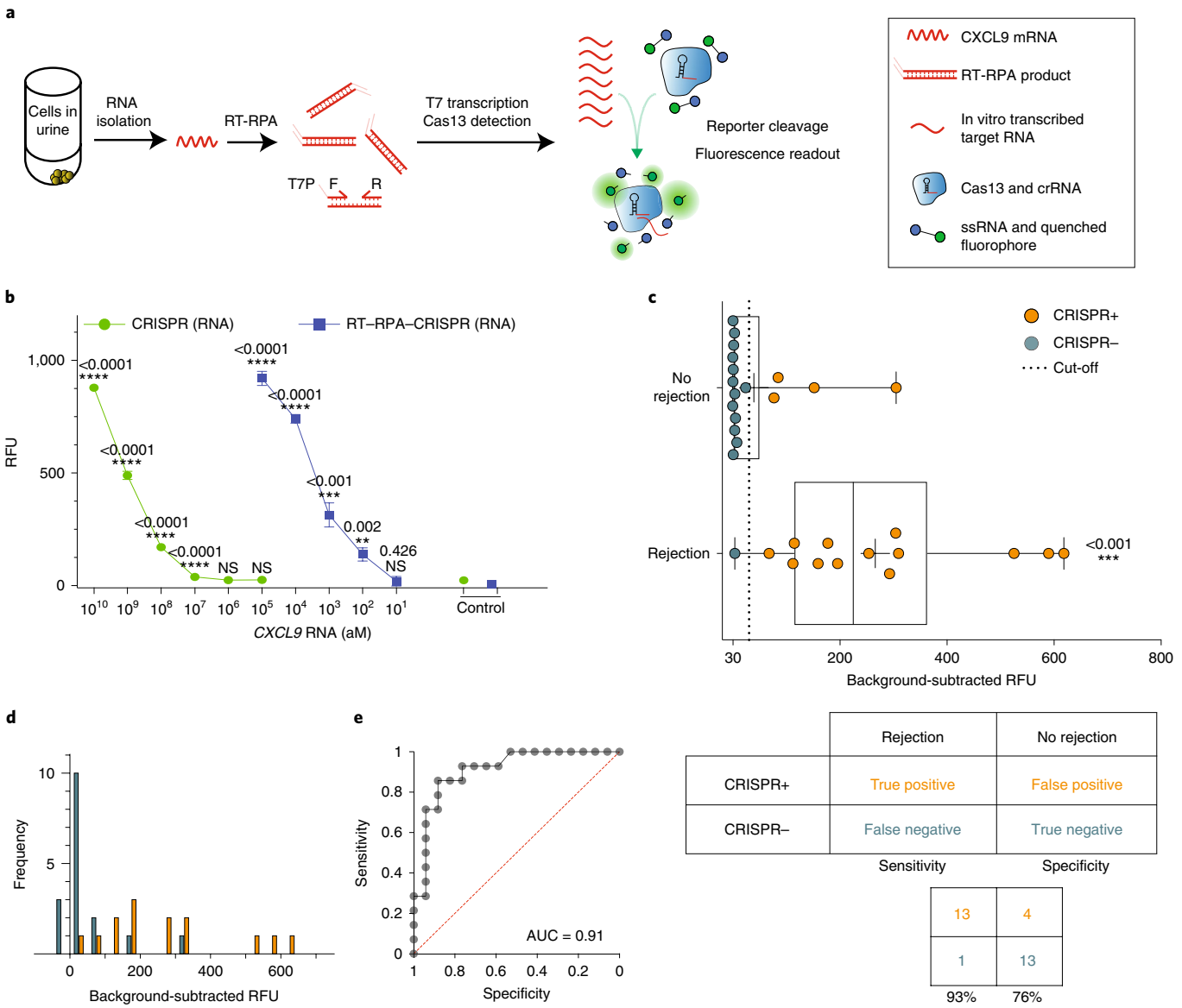

Fig. 3 | CRISPR-based diagnostics can detect *CXCL9* mRNA as an indicator for acute cellular rejection. a, Schematic illustrating the assay. After isolation of RNA from urine, *CXCL9* mRNA is amplified by RT-RPA. T7 transcription of the RPA products allows for Cas13 detection of target RNA and subsequent collateral cleavage of reporter molecules. **b**, Detection of *CXCL9* synthetic RNA with Cas13 only (green) or Cas13 with RT-RPA–CRISPR (blue). Data are mean ± s.d. of three independent reactions. The experiment was repeated three times. **c**, Top: CRISPR-based detection of *CXCL9* mRNA in urine sample. The dashed line indicates the cut-off separating CRISPR-positive samples (orange) from CRISPR-negative samples (blue). Rejection status was determined by kidney biopsy. In box plots, the centre line is the median, boxes encompass second and third quartiles, whiskers represent the range of the data and crosses show the mean. Each symbol represents an independent patient sample, $n = 14$ rejection samples, $n = 17$ no-rejection samples. Bottom: confusion matrix for detection of rejection by CRISPR-based *CXCL9* test. **d**, Frequency distribution of signal intensities for the no-rejection (blue) and rejection (orange) groups. **e**, Area under the receiver-operating-characteristic curve (AUC), assessing the accuracy of CRISPR-based rejection diagnostics (AUC of 1 indicates perfect discriminatory value; 0.5 or less indicates no discriminatory value). Difference from control assessed by two-tailed Student's *t*-test. NS, not significant; $^{*}P < 0.05$, $^{**}P < 0.01$, $^{***}P < 0.001$ and $^{****}P < 0.0001$ (**b**,**c**).

the attomolar range. We set the relative band-intensity cut-off discriminating a positive from a negative test result to 0.5, which corresponded to an interpolated concentration of 2.3 aM for the CMV standard and 0.5 aM for the BKV standard.

Using this protocol, we were able to detect CMV (Fig. 4d) and BKV (Fig. 4e) at different concentrations in patient samples. Although faint test bands were observable at very low concentrations, they were below the band-intensity cut-off and thus classified as negative. Further, lateral-flow-based CRISPR diagnostics successfully identified BKV infection in a 58-yr-old male kidney-transplant recipient who was admitted for graft dysfunction. A kidney biopsy demonstrated BKV nephropathy and qPCR confirmed high viral BKV titres in the blood.

After treatment, we could not detect BKV using CRISPR–Cas13; this result was validated by the absence of viral DNA in qPCR (Fig. 4f).

To assess lateral-flow signal variability over time, we tested the same ten BKV-positive or -negative patient samples on three different days (Fig. 4g,h). We observed that all BKV-negative samples were consistently below the band-intensity cut-off on all three days, whereas all BKV positive samples were above the

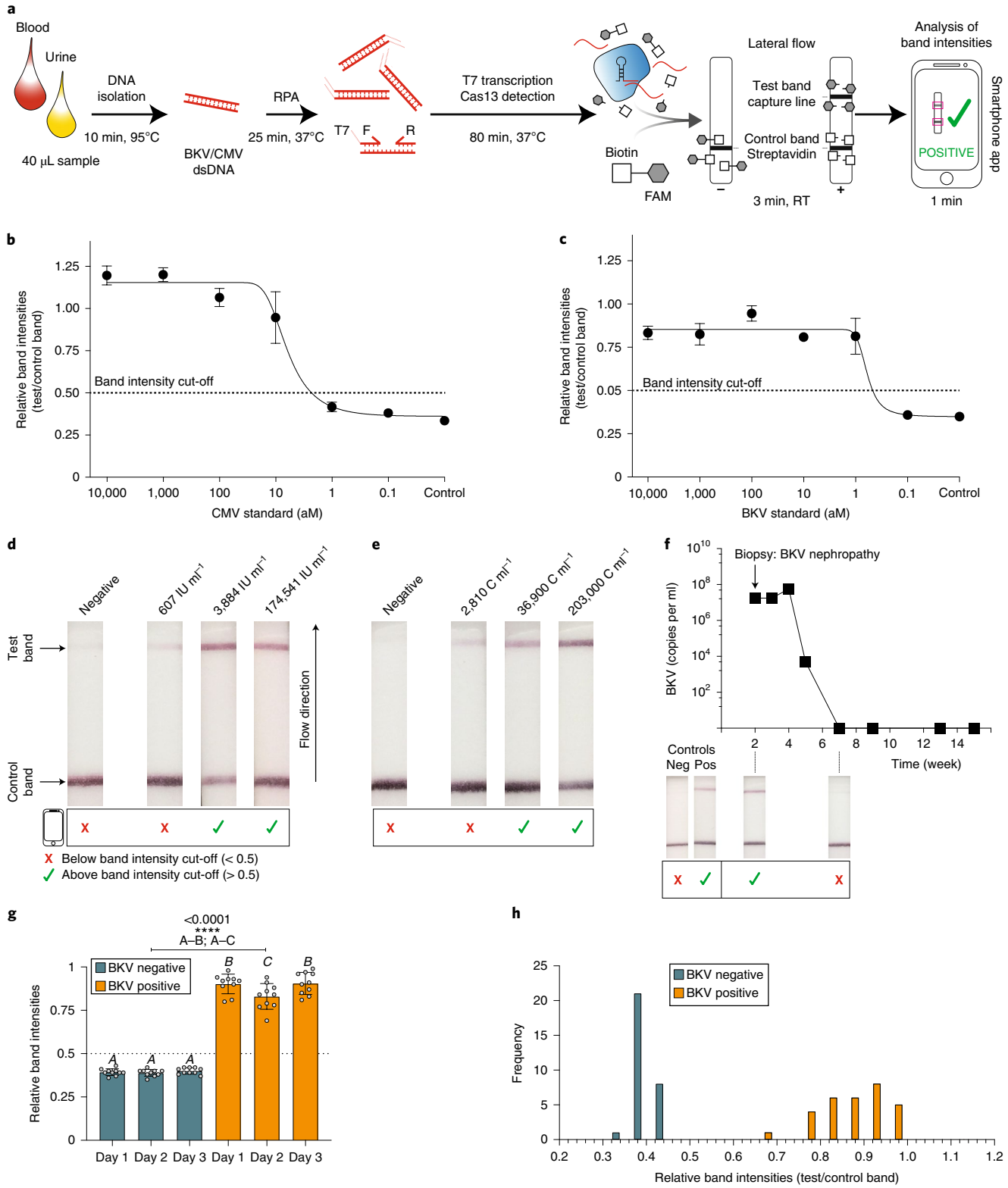

Fig. 4 | Lateral flow enables detection of viral DNA (BKV, CMV) for point-of-care testing. a, Schematic illustrating the assay. **b**,**c**, Lateral-flow-based detection of CMV (**b**) and BKV (**c**) synthetic standards at the indicated concentrations. Data are mean ± s.d. of three independent reactions. Dashed line indicates the band-intensity cut-off discriminating a positive assay result from a negative. **d**,**e**, Detection of CMV (**d**) and BKV (**e**) in patient plasma samples with lateral-flow strips. Viral copy number was measured by qPCR. The boxed areas below indicate whether smartphone-based band detection was positive (green tick) or negative (red cross). **f**, Top: monitoring of BKV infection (BKV viral load quantified by qPCR) over the indicated time period in a transplant recipient with BKV nephropathy. Bottom: lateral-flow-based detection of BKV in urine at the indicated time points. Neg, negative control; pos, positive control. **g**, Signal variability of the lateral-flow assay detecting the same ten BKV negative or positive patient samples on three different days. Data are mean ± s.d., $n = 10$ samples. Letters indicate groups that are significantly different from each other; one-way ANOVA and Tukey's multiple comparisons test. **h**, Histograms indicating the frequency distribution of lateral-flow signals shown in **g**.

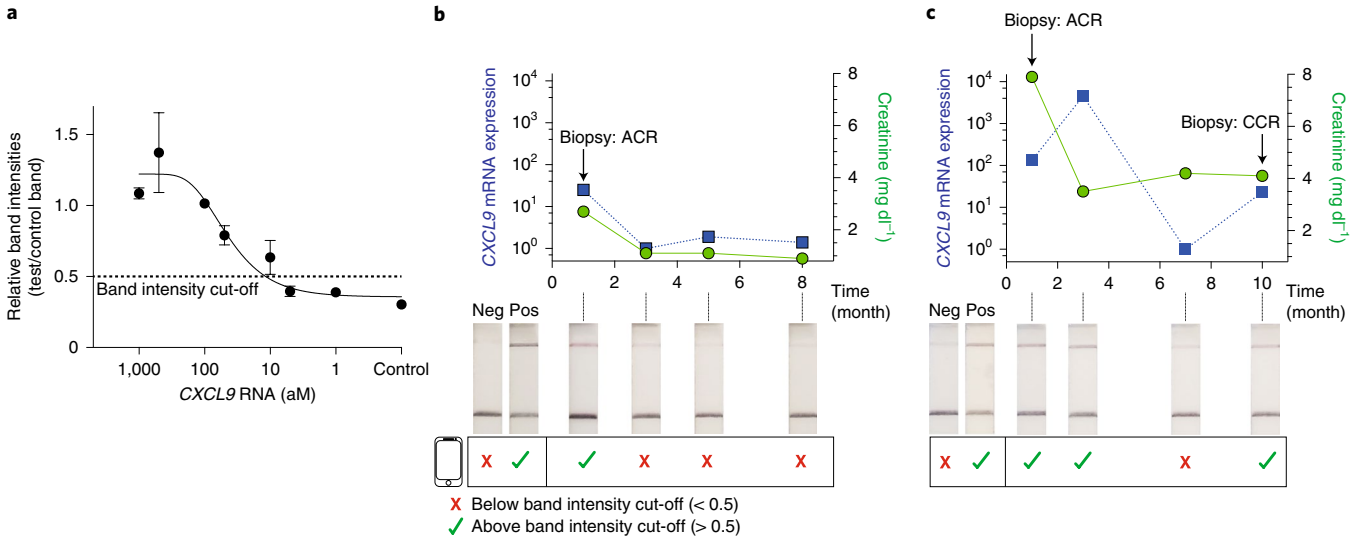

Fig. 5 | Monitoring of *CXCL9* mRNA levels with lateral flow. a, Lateral-flow-based detection of *CXCL9* synthetic RNA at the indicated concentrations. Dashed line indicates the band-intensity cut-off discriminating a positive from a negative assay result. Data are mean ± s.d. of three independent reactions. **b**,**c**, Monitoring of two kidney-transplant recipients undergoing organ rejection and treatment. Top: blue squares and left axis, *CXCL9* mRNA expression measured by quantitative PCR with reverse transcription (RT–qPCR); green circles and right axis, serum creatinine; ACR, acute cellular rejection; CCR, chronic cellular rejection. Arrows indicate time points of kidney biopsies. Bottom: lateral-flow assays for *CXCL9* mRNA in urine.

cut-off. This suggested a low variability of background noise and band intensities.

We also assessed the influence of incubation time and temperature on lateral-flow band intensity for two different concentrations of the CMV synthetic standard. For the negative control, the relative band intensity stayed below the 0.5 cut-off regardless of the incubation time, in line with our previous results (Supplementary Fig. 4a,b). When detecting 5 or 500 aM of CMV synthetic DNA, we observed a time-dependent increase of band intensities. Notably, we could observe band-intensity values above the cut-off only after 60 min, indicating that our assay incubation time could be further reduced. For different reaction temperatures ranging between 21 °C and 39 °C, we again observed band-intensity ratios below 0.5 for the negative control (Supplementary Fig. 4c,d). While room temperature (21 °C) was sufficient to detect 5 or 500 aM of CMV synthetic standard, higher temperatures correlated with higher band intensities. These results indicate that reaction time and temperature are important variables if a quantitative lateral-flow readout is the goal. By contrast, highly consistent background noise irrespective of daily variation, incubation time and temperature enables a robust qualitative assay.

We further optimized the combination of RPA, T7 transcription and Cas13 in one reaction ('one-pot reaction'; Supplementary Fig. 5a) by testing different reaction buffers and nucleotide ratios (Supplementary Fig. 5b–d). Using this optimized one-pot reaction, we achieved BKV detection in the attomolar range (Supplementary Fig. 5e).

Detection of *CXCL9* mRNA levels with lateral flow enables monitoring of kidney rejection and treatment response. Next, we sought to apply the lateral-flow-based assay for the detection of *CXCL9* mRNA indicative of acute cellular kidney rejection. Similar to the detection of viral DNA, lateral flow enabled robust detection of *CXCL9* synthetic RNA (Fig. 5a) down to the attomolar range. Using nonlinear regression analysis, we determined that a concentration of 12 aM corresponded to the 0.5 band-intensity cut-off.

To investigate the power of our CRISPR-based readout for rejection monitoring, we selected two patients experiencing allograft cellular rejection as confirmed by biopsy, from whom we had at least three prospective samples after the rejection event (Fig. 5b,c). Patient 1 (Fig. 5b) had an acute cellular rejection (Banff IIA) and showed a good response to treatment with thymoglobulin and pulse methylprednisolone, achieving full clinical recovery. This was reflected by a strong downregulation of *CXCL9* mRNA levels as observed by qPCR and return to their baseline serum creatinine (0.9 mg dl^{-1}). CRISPR-based testing detected *CXCL9* mRNA during rejection only, and the patient was *CXCL9* negative after treatment completion.

By contrast, Patient 2 (Fig. 5c) had an episode of acute cellular rejection (Banff IIA) with partial improvement of creatinine after treatment (serum creatinine 3.5 mg dl^{-1}, down from 7.9 mg dl^{-1}). Levels of *CXCL9* mRNA in the urine were reduced initially, but increased again 7 months after treatment, and repeat biopsy revealed chronic active cellular rejection. Overall, monitoring of urine *CXCL9* mRNA levels may be a useful tool to assess response to rejection treatment, though further validation in a larger trial is needed.

Discussion

Fast and cost-effective POC testing should enable early diagnosis and greater accessibility for patients in low-resource settings, including the opportunity for self-monitoring. Here, we applied CRISPR–Cas13 diagnostics to detect infection with CMV and BKV in samples from recipients of kidney transplants. We extended the use of SHERLOCK for the detection of *CXCL9* mRNA, a biomarker of acute cellular rejection of kidney transplants. Together, these developments may enable the cost-effective (Supplementary Table 3) monitoring of patients at risk of opportunistic infection and serve as a tool for earlier detection of rejection and monitoring after organ transplantation.

BKV and CMV are among the most common opportunistic infections after solid-organ transplantation, and are associated with substantial morbidity[21]. However, clinical presentation is variable in transplanted patients and BKV infection frequently presents without clinical symptoms except an increase in creatinine, which indicates already established BKV nephropathy. Blood testing for

BKV and CMV viral load is recommended but is not uniformly performed in all centres due to cost limitations, particularly in developing countries. Here, our high-sensitivity, low-cost POC assay could allow for more frequent testing.

Rejection is the leading cause of chronic allograft loss. However, rejection is usually detected late since serum creatinine is a delayed marker of allograft injury. Furthermore, the diagnosis of acute rejection currently requires a renal biopsy–an invasive process that is limited by sampling error and assessment variability[22]. In order to detect graft injury earlier, some centres perform surveillance kidney biopsies at prespecified time points after transplantation[23]. However, these procedures are associated with major risks for patients, such as bleeding, and high costs (about US$3,500 per biopsy, which includes the procedure and the pathological analyses of the kidney specimen). Therefore, a sensitive and non-invasive assay such as CRISPR–Cas13-based *CXCL9* mRNA testing could enable more frequent testing and thereby achieve earlier detection of graft rejection, allowing timely diagnosis and treatment.

Currently, screening for donor-specific human leukocyte antigen antibodies (DSA) is performed in patients with concern for antibody-mediated rejection. All patients included in our study tested negative for DSA. Screening prospectively for DSA in all patients is not uniformly performed, in part due to lack of specificity of DSA to antibody-mediated rejection.

Besides DSA screening, two blood tests that detect the fraction of donor-derived cell-free DNA have become clinically available in kidney transplantation to monitor for rejection[24,25]. While these assays have shown promising results, they still require a visit to the clinic to draw blood and shipping of the material to outside laboratories for processing and analysis, and they have a high price tag of US$2,821 per test (https://www.sec.gov/Archives/edgar/data/1217234/000156459018006584/cdna-10k_20171231.htm). This high price limits the frequency of testing and also prevents the use of this test in resource-limited settings. The advantages of our rejection assay are its low cost, its high sensitivity and its use of urine compared to blood. Since elevation of *CXCL9* mRNA in the urine can be detected weeks before elevation of creatinine due to rejection[26], urine *CXCL9* mRNA monitoring may represent a promising technique for earlier rejection detection as well as post-treatment monitoring. Lastly, the development of a smartphone application to enable simple and fast interpretation of the lateral-flow assay allows for sharing of results directly with the provider, leading to a convenient way of monitoring patients between clinical appointments.

Our test was mainly aimed at qualitative detection of CMV, BKV and *CXCL9* mRNA at clinically relevant concentrations. However, in many clinical situations, precise quantification of the viral load and changes in biomarker levels are useful. Future iterations of this protocol should, therefore, include quantification strategies and may build on recent protocols demonstrating semi-quantitative readouts of CRISPR diagnostics[3]. This would also strengthen the power of CRISPR-based diagnostics, since it could enable the detection of subtle changes as a deviation from an individualized baseline. Moreover, although most steps could be optimized for POC testing, sample isolation for the detection of mRNA still required a column-based approach. Thus, further work will involve optimizing the protocol for simplified mRNA-isolation procedures. In addition, heating represents an essential step in our current sample-processing protocol using HUDSON. Thus, the integration of POC heating devices using chemical[27] or electromagnetic[28] heating might facilitate handling for the primary care provider or patient. Finally, inclusion of more patient samples and prospective analysis will allow for systematic comparison with current clinical practice. While we have focused this study on cellular-mediated rejection, the most frequent rejection affecting kidney-transplant recipients, our next steps will include expanding and validating our rejection assay for the detection of antibody-mediated rejection and its potential complementary role to DSA testing[29,30].

In summary, this work shows the application of CRISPR–Cas13 for the detection of rejection and opportunistic infection in kidney transplantation. This technology could be applied to other solid-organ transplants as well as immune-mediated kidney diseases such as lupus nephritis. On the basis of its low cost, ease of use and speed, this assay could enable frequent testing and earlier diagnosis. The next steps in order to advance clinical implementation include studies to validate these findings and to demonstrate the clinical utility of this assay in regard to long-term outcomes of kidney-transplant recipients.

Methods

Lateral-flow reactions. Twenty microlitres of the SHERLOCK reaction containing the lateral-flow reporter oligonucleotide at 1 μM (sequence in Supplementary Table 4) were mixed with 80 μl of Hybridetect Assay buffer, followed by insertion of lateral-flow sticks (Milenia Hybridetect1, TwistDx) and incubation for 3 min at room temperature, according to the manufacturer's instructions, before images were taken.

Image analysis of lateral-flow reactions. The relative band intensities of each of the lateral-flow sticks were measured using ImageJ software (National Institutes of Health). The relative band intensity was calculated as the mean grey value of the test band/mean grey value of the control band. Images were first converted to 8 bit and inverted, before highlighting the band region and measuring its mean grey value.

Lateral-flow quantification app. The lateral-flow quantification algorithm was implemented using the opencv package v.4.1.1 in Python v.3.7.4. In brief, images uploaded to the app are automatically converted to greyscale and the colours are inverted. The resultant image is then subjected to a Gaussian blur to remove outlier pixels that may result in artefactual bright spots. A threshold is then applied to accentuate bright spots. Connected-component analysis is then used to isolate regions corresponding to the control and sample bands. These bands are then identified and quantified by calculating the mean intensity of each band. If the sample band cannot be identified due to weak intensity, the sample band's location is estimated by scanning for bright areas in the upper portion of the lateral-flow stick using the control band as a perspective scale. The ratio of the sample to control band is then calculated and displayed to the user. The Android app was developed with Android Studio v.3.5.1 (Google) with Java 8 and Gradle v.5.4.1 (Supplementary Video 1). To provide a clean user interface, the main screen was limited to three buttons: (1) upload new pictures, (2) specify the target of the assay (that is, CMV, BKV or *CXCL9*), and (3) initiate image analysis. The image-upload process requests read permissions to the phone's photo gallery. Image analysis allows two options, with the faster analysis scaling down the image to 50% lower resolution for more rapid results. The pixel array is passed to a Python back end through Chaquopy v.6.3.0, a Python software development kit for Android.

Sample preparation. Patient samples containing CMV or BKV were prepared as indicated, either with the previously described HUDSON protocol[2] or the QIAamp MinElute Virus Spin Kit (Qiagen), according to the manufacturer's instructions. For HUDSON processing, the samples were heated for 10 min at 95 °C in the presence of 100 mM tris(2-carboxyethyl)phosphine (Fisher Scientific) and 1 mM EDTA (Fisher Scientific). For *CXCL9* mRNA detection, 45 ml urine was centrifuged for 30 min at 2000*g* at 4 °C, followed by washing of the pellet with PBS and resuspension in 200 μl RNAlater (Qiagen). All samples were aliquoted and stored at −80 °C. RNA was isolated using the RNeasy Micro Kit (Qiagen) and the PureLink RNA Mini Kit (Invitrogen), following the manufacturers' instructions.

Production of crRNAs and LwaCas13a. LwaCas13a was produced by Genscript (Piscataway). crRNAs were synthesized using the HiScribe T7 Quick High Yield RNA Synthesis Kit (NEB) according to the manufacturer's instructions, with the T7 promoter containing annealed oligonucleotides. Reactions were incubated for 16 h at 37 °C, digested using DNAse (New England Biolabs) and purified using the RNA Clean & Concentrator-25 kit (ZymoResearch).

RPA primer and crRNA design. Genetically conserved regions in the BKV and CMV genome were identified using publicly accessible databases (Virus Pathogen Resource and NCBI). Alignments were performed using MAFFT[31] and visualized with Jalview[32]. RPA primer design was done using the PRIMER-BLAST tool with previously described settings[3]. *CXCL9* RPA primers were designed to be in proximity to previously published qPCR primers[18]. For each region to be amplified, optimal primer pairs were identified by forward and reverse primer screens. Primer concentrations were optimized by testing different forward and reverse primer concentrations in a dilution matrix. crRNAs, 28 nucleotides complementary

to the target region, were designed as previously described[1,3] and tested for their performance with each RPA-primer pair. The sequences, including spacer, direct repeat and T7 promoter, are shown in Supplementary Table 4.

RT–qPCR. RNA isolation, reverse transcription and qPCR were performed as previously described[18]. In brief, we reverse transcribed RNA using the TaqMan Reverse Transcription kit (ThermoFisher) with random hexamers. The qPCR was performed using cDNA without pre-amplification. qPCR reactions were set up as previously described[18]. All reactions were performed in duplicate, using the Applied Biosystems StepOne Plus real-time PCR system (ThermoFisher). In vitro transcribed RNA for *CXCL9* served as a standard (sequences in Supplementary Table 4). For expression analysis, we employed the comparative C_T method[33] for quantification relative to 18 S RNA (Supplementary Fig. 3a) or used absolute quantification on the basis of a *CXCL9* standard curve (Fig. 5b,c). Expression levels are presented on a logarithmic scale relative to the control, whose average expression was set to 1.

RPA reactions. For RPA reactions, the TwistAmp Liquid Basic kit (TwistDx) was used according to the manufacturer's instructions, with the following modifications. Primer concentrations were 120 nM for the forward primer and 480 nM for the reverse primer. The total reaction volume was 20 µl, with a final concentration of dNTPs at 7.2 mM (total) and magnesium acetate at 8 mM. RPA reactions were incubated at 37 °C for 50 min. For RT–RPA reactions, forward and reverse primers were used at 480 nM each and magnesium acetate was used at 14 mM. One microlitre GoScript reverse transcriptase (Promega) was added to a 20 µl reaction containing DL-dithiothreitol solution (Sigma-Aldrich) at a final concentration of 19 mM. The primer–RNA mix was pre-incubated at 65 °C for 10 min and the RT–RPA reaction was performed at 42 °C for 60 min.

Cas13 reactions. Detection of RPA or RT–RPA-amplified targets was performed as described previously[1–3] with minor modifications. NEB buffer 2 (NEB) served as cleavage buffer at a final concentration of 1×. Three microlitres of RPA or RT–RPA product were used in a 20 µl Cas13 reaction. Fluorescence (485 nm excitation, 520 nm emission) was measured on a plate reader (SpectraMax M5, Molecular Devices) every 5 min for up to 3 h at 37 °C.

One-pot reaction. One-pot RPA–CRISPR reactions were performed with murine RNAse Inhibitor (NEB) at 1 U µl^{-1}, Cas13 at 45 nM, crRNA at 22.5 nM, RNAse Alert V2 (Thermofisher) at 125 nM, human background RNA (from 293 T cells) at 1.25 ng µl^{-1}, T7 polymerase (Lucigen) at 0.6 µl per 20 µl, dNTPs at 1.8 mM (total), rNTPs at 0.5 mM (each), magnesium acetate at 16 mM and the buffers of the RPA TwistAmp Liquid Basic kit (2×, 10× and 20× buffers) at 1X final concentrations.

Diagnostic BKV and CMV quantitative PCR. De-identified patient samples were provided by the Crimson Core at Brigham and Women's Hospital (BWH). Quantification of BKV and CMV viral load were performed at the Clinical Laboratory Improvement Amendments-certified diagnostic core facility at BWH. In brief, BKV viral load samples were processed using the Luminex Aries instrument (Luminex) and a laboratory-developed protocol for a probe-free, two-primer, real-time PCR system. Following amplification, a thermal melt was performed. The system software allows for a quantitation template, developed using a standard curve calibrated against the first World Health Organization International Standard for BKV, to be applied to raw data for production of a quantitative value, reported in copies per ml (C ml^{-1}). CMV viral load samples were processed using the Roche Cobas AmpliPrep/Cobas TaqMan CMV Test on the Roche-docked Cobas AmpliPrep/TaqMan instrument. This is a real-time PCR system that automates specimen preparation, PCR amplification, target detection and quantitation. Results are reported in International Units per ml (IU ml^{-1}).

Patient populations. For the CMV and BKV studies, de-identified samples collected for clinical testing for CMV and BKV viremia at the BWH were provided by the Crimson Core at BWH. Clinical reported results for CMV and BK viremia were then compared to CRISPR–Cas13-diagnostics results. For the rejection and BKV nephropathy samples, patients were recruited prior to a kidney-transplant biopsy to investigate an elevation of creatinine at BWH. Prospective sample collection was also performed in few kidney-transplant recipients between January 2019 and June 2019. Samples started to be collected after one month of transplantation to avoid the effect of surgery and ischemic time. Samples were then collected according to clinical visits for 3–5 collections within the first year of transplant. The kidney-transplant cohort is representative of kidney-transplant recipients in this geographical location and at a tertiary academic hospital.

Statistics. CRISPR reactions were expressed as the mean of at least three independent reactions ± s.d. or s.e.m., as indicated in the figure legends. For statistical analysis, comparisons of patients with rejection and controls were conducted by unpaired two-tailed Student's *t*-test. Multiple group comparisons were conducted using one-way ANOVA and Tukey's multiple comparisons test. Comparisons of one control group to multiple others groups were performed using one-way ANOVA and Dunnett's multiple comparisons test. Statistical analyses were performed using GraphPadPrism 7.

Study design and participants. The study was approved by the Institutional Review Board at BWH (2017P000298), and the procedures followed were in accordance with institutional guidelines. In this observational study, a total of 31 kidney-transplant recipients were enrolled, and informed consent was obtained from all study participants (Supplementary Tables 1 and 2). Urine samples were collected from patients undergoing kidney biopsy for clinical indications. The cohort of samples was then selected on the basis of the presence of cellular rejection or no rejection on biopsy findings. For the prospective analyses, samples were provided by a cohort from Montefiore Medical Center, Bronx, NY (Montefiore/Einstein Institutional Review Board (09-06-174). In brief, longitudinal samples were collected at the following time points: 0–3 months, 6–9 months and 9–12 months after transplant or when clinical biopsy was performed). Selection of patients was on the basis of availability of at least three samples collected either before or after a rejection event that was classified as rejection Banff IA or higher.

Ethics. We have complied with all relevant ethical regulations. The patient samples used in this study were obtained from the clinical study Biomarkers in Kidney Transplantation, which was approved by Partners Human Research Committee (2017P000298/PHS). We have obtained written informed consent from all participants.

Reporting Summary. Further information on research design is available in the Nature Research Reporting Summary linked to this article.

Data availability

The authors declare that the data supporting the findings of this study are available within the paper and its Supplementary information files. The raw and analysed datasets generated during the study are available for research purposes from the corresponding authors on reasonable request, and the availability of raw patient data is subject to approval from the Institutional Review Board.

Code availability

The lateral-flow quantification app code is available at https://github.com/jackievaleri/lateral_flow_quantification_app.

Received: 21 October 2019; Accepted: 6 March 2020;
Published online: 13 April 2020

References

1. Gootenberg, J. S. et al. Nucleic acid detection with CRISPR–Cas13a/C2c2. *Science* **356**, 438–442 (2017).
2. Myhrvold, C. et al. Field-deployable viral diagnostics using CRISPR–Cas13. *Science* **448**, 444–448 (2018).
3. Gootenberg, J. S. et al. Multiplexed and portable nucleic acid detection platform with Cas13, Cas12a, and Csm6. *Science* **360**, 439–444 (2018).
4. Chen, J. S. et al. CRISPR–Cas12a target binding unleashes indiscriminate single-stranded DNase activity. *Science* **360**, 436–439 (2018).
5. Harrington, L. B. et al. Programmed DNA destruction by miniature CRISPR–Cas14 enzymes. *Science* **362**, 839–842 (2018).
6. Pardee, K. et al. Rapid, low-cost detection of Zika virus using programmable biomolecular components. *Cell* **165**, 1255–1266 (2016).
7. Haijan, R. et al. Detection of unamplified target genes via CRISPR–Cas9 immobilized on a graphene field-effect transistor. *Nat. Biomed. Eng.* **3**, 427–437 (2019).
8. Wu, Y., Liu, S.-X., Wang, F. & Zeng, M.-S. Room temperature detection of plasma Epstein–Barr virus DNA with CRISPR–Cas13. *Clin. Chem.* **65**, 591–592 (2019).
9. Lamb, K. E., Lodhi, S. & Meier-Kriesche, H.-U. Long-term renal allograft survival in the United States: a critical reappraisal. *Am. J. Transplant.* **11**, 450–462 (2011).
10. Tullius, S. G. & Rabb, H. Improving the supply and quality of deceased-donor organs for transplantation. *N. Engl. J. Med.* **378**, 1920–1929 (2018).
11. Wekerle, T., Segev, D., Lechler, R. & Oberbauer, R. Strategies for long-term preservation of kidney graft function. *Lancet* **389**, 2152–2162 (2017).
12. Ross, S. A., Novak, Z., Pati, S. & Boppana, S. B. Overview of the diagnosis of cytomegalovirus infection. *Infect. Disord. Drug Targets* **11**, 466–474 (2011).
13. Randhawa, P. et al. Correlates of quantitative measurement of BK polyomavirus (BKV) DNA with clinical course of BKV infection in renal transplant patients. *J. Clin. Microbiol.* **42**, 1176–1180 (2004).
14. Fishman, J. A. Infection in organ transplantation. *Am. J. Transplant.* **17**, 856–879 (2017).
15. Sepkowitz, K. A. Opportunistic infections in patients with and patients without acquired immunodeficiency syndrome. *Clin. Infect. Dis.* **34**, 1098–1107 (2002).
16. Sundsfjord, A. et al. BK and JC viruses in human immunodeficiency virus type 1-infected persons: prevalence, excretion, viremia, and viral regulatory regions. *J. Infect. Dis.* **169**, 485–490 (1994).

17. Jackson, J. A. et al. Urinary chemokines CXCL9 and CXCL10 are noninvasive markers of renal allograft rejection and BK viral infection. *Am. J. Transplant.* **11**, 2228–2234 (2011).
18. Hricik, D. E. et al. Multicenter validation of urinary CXCL9 as a risk-stratifying biomarker for kidney transplant injury. *Am. J. Transplant.* **13**, 2634–2644 (2013).
19. Schaub, S. et al. Urinary CXCL9 and CXCL10 levels correlate with the extent of subclinical tubulitis. *Am. J. Transplant.* **9**, 1347–1353 (2009).
20. Rabant, M. et al. Early low urinary CXCL9 and CXCL10 might predict immunological quiescence in clinically and histologically stable kidney recipients. *Am. J. Transplant.* **16**, 1868–1881 (2016).
21. Fishman, J. A. Infection in solid-organ transplant recipients. *N. Engl. J. Med.* **357**, 2601–2614 (2007).
22. El-Zoghby, Z. M. et al. Identifying specific causes of kidney allograft loss. *Am. J. Transplant.* **9**, 527–535 (2009).
23. Henderson, L. K., Nankivell, B. J. & Chapman, J. R. Surveillance protocol kidney transplant biopsies: their evolving role in clinical practice. *Am. J. Transplant.* **11**, 1570–1575 (2011).
24. Bloom, R. D. et al. Cell-free DNA and active rejection in kidney allografts. *J. Am. Soc. Nephrol.* **28**, 2221–2232 (2017).
25. Sigdel, T. K. et al. Optimizing detection of kidney transplant injury by assessment of donor-derived cell-free DNA via massively multiplex PCR. *J. Clin. Med.* **8**, E19 (2018).
26. Hricik, D. E. et al. Adverse outcomes of tacrolimus withdrawal in immune–quiescent kidney transplant recipients. *J. Am. Soc. Nephrol.* **26**, 3114–3122 (2015).
27. Curtis, K. A. et al. Isothermal amplification using a chemical heating device for point-of-care detection of HIV-1. *PLoS ONE* **7**, e31432 (2012).
28. Ahn, M.-H., Baek, S.-K., Min, J. & Park, J.-H. A portable electromagnetic induction heating device for point-of-care diagnostics. *BioChip J.* **10**, 208–214 (2016).
29. Parajuli, S. et al. Donor-specific antibodies in the absence of rejection are not a risk factor for allograft failure. *Kidney Int. Rep.* **4**, 1057–1065 (2019).
30. Schinstock, C. A. et al. The value of protocol biopsies to identify patients with de novo donor-specific antibody at high risk for allograft loss. *Am. J. Transplant.* **17**, 1574–1584 (2017).
31. Katoh, K. & Standley, D. M. MAFFT multiple sequence alignment software version 7: improvements in performance and usability. *Mol. Biol. Evol.* **30**, 772–780 (2013).
32. Waterhouse, A. M., Procter, J. B., Martin, D. M. A., Clamp, M. & Barton, G. J. Jalview Version 2—a multiple sequence alignment editor and analysis workbench. *Bioinformatics* **25**, 1189–1191 (2009).
33. Schmittgen, T. D. & Livak, K. J. Analyzing real-time PCR data by the comparative C_T method. *Nat. Protoc.* **3**, 1101 (2008).

Acknowledgements

We thank R. Zaffini from viral microbiology (BWH) for helpful discussion about BKV testing and qPCR; the Crimson Core at BWH for providing samples from patients with CMV and BKV; and H. de Puig, N. Angenent-Mari, A. Dy and X. Tan for helpful discussions. M.M.K. was supported by the German Academy of Sciences, Leopoldina (LPDS 2018-01), the Clinician Scientist Program Berta–Ottenstein of the Faculty of Medicine, University of Freiburg, Germany and the Emmy Noether Programme (KA5060/1-1). M.A.A. was supported by a National Science Foundation graduate research fellowship (award no. 1122374). V.K. was supported by the DFG (grant no. 403877094). J.J.C. was supported by MIT's Center for Microbiome Informatics and Therapeutics, the Paul G. Allen Frontiers Group and the Wyss Institute.

Author contributions

M.M.K., L.V.R. and J.J.C. designed the study. M.M.K., M.A.A., A.C.H., I.L. and R.G. performed experiments. J.A.V. and M.A.A. programmed the smartphone app, and V.K. contributed to the design and analysis of experiments. L.V.R. and E.A. provided clinical samples. F.M.M. and J.A. advised on the collection and testing of clinical specimens. All authors contributed to the writing of the manuscript and interpretation of data.

Competing interests

A patent application related to this work is pending. J.J.C. is co-founder and director of Sherlock Biosciences.

Additional information

Supplementary information is available for this paper at https://doi.org/10.1038/s41551-020-0546-5.

Correspondence and requests for materials should be addressed to L.R. or J.J.C.

nature research

Corresponding author(s): James J. Collins, Leonardo Riella

Last updated by author(s): Mar 4, 2020

Reporting Summary

Nature Research wishes to improve the reproducibility of the work that we publish. This form provides structure for consistency and transparency in reporting. For further information on Nature Research policies, see Authors & Referees and the Editorial Policy Checklist.

Statistics

For all statistical analyses, confirm that the following items are present in the figure legend, table legend, main text, or Methods section.

n/a	Confirmed	
☐	☒	The exact sample size (*n*) for each experimental group/condition, given as a discrete number and unit of measurement
☐	☒	A statement on whether measurements were taken from distinct samples or whether the same sample was measured repeatedly
☐	☒	The statistical test(s) used AND whether they are one- or two-sided *Only common tests should be described solely by name; describe more complex techniques in the Methods section.*
☒	☐	A description of all covariates tested
☒	☐	A description of any assumptions or corrections, such as tests of normality and adjustment for multiple comparisons
☐	☒	A full description of the statistical parameters including central tendency (e.g. means) or other basic estimates (e.g. regression coefficient) AND variation (e.g. standard deviation) or associated estimates of uncertainty (e.g. confidence intervals)
☐	☒	For null hypothesis testing, the test statistic (e.g. *F*, *t*, *r*) with confidence intervals, effect sizes, degrees of freedom and *P* value noted *Give P values as exact values whenever suitable.*
☒	☐	For Bayesian analysis, information on the choice of priors and Markov chain Monte Carlo settings
☒	☐	For hierarchical and complex designs, identification of the appropriate level for tests and full reporting of outcomes
☒	☐	Estimates of effect sizes (e.g. Cohen's *d*, Pearson's *r*), indicating how they were calculated

Our web collection on statistics for biologists contains articles on many of the points above.

Software and code

Policy information about availability of computer code

Data collection	Microsoft Office 2019
Data analysis	MAFFT version 7; Jalview 2.10.3b1; Prism7

For manuscripts utilizing custom algorithms or software that are central to the research but not yet described in published literature, software must be made available to editors/reviewers. We strongly encourage code deposition in a community repository (e.g. GitHub). See the Nature Research guidelines for submitting code & software for further information.

Data

Policy information about availability of data

All manuscripts must include a data availability statement. This statement should provide the following information, where applicable:

- Accession codes, unique identifiers, or web links for publicly available datasets
- A list of figures that have associated raw data
- A description of any restrictions on data availability

The authors declare that the data supporting the findings of this study are available within the paper and its supplementary information files. The raw and analysed datasets generated during the study are available for research purposes from the corresponding authors on reasonable request, and the availability of raw patient data is subject to approval from the Institutional Review Board.

Field-specific reporting

Please select the one below that is the best fit for your research. If you are not sure, read the appropriate sections before making your selection.

☒ Life sciences ☐ Behavioural & social sciences ☐ Ecological, evolutionary & environmental sciences

For a reference copy of the document with all sections, see nature.com/documents/nr-reporting-summary-flat.pdf

Life sciences study design

All studies must disclose on these points even when the disclosure is negative.

Sample size	Sample sizes were chosen on the basis of anticipated variability between measures.
Data exclusions	No data were excluded.
Replication	Experiments were repeated at least twice. All attempts at replication were successful.
Randomization	Patient samples for the testing of BKV and CMV were randomly selected by the CRIMSON core at Brigham & Women's Hospital. Patient samples for rejection testing were randomly selected from groups of patients with biopsy-proven acute cellular rejection and of control patients with either stable kidney function or absence of rejection in biopsy.
Blinding	Samples were not blinded.

Reporting for specific materials, systems and methods

We require information from authors about some types of materials, experimental systems and methods used in many studies. Here, indicate whether each material, system or method listed is relevant to your study. If you are not sure if a list item applies to your research, read the appropriate section before selecting a response.

Materials & experimental systems

n/a	Involved in the study
☒	☐ Antibodies
☒	☐ Eukaryotic cell lines
☒	☐ Palaeontology
☒	☐ Animals and other organisms
☐	☒ Human research participants
☐	☒ Clinical data

Methods

n/a	Involved in the study
☒	☐ ChIP-seq
☒	☐ Flow cytometry
☒	☐ MRI-based neuroimaging

Human research participants

Policy information about studies involving human research participants

Population characteristics	For the cohort of CMV and BKV samples, deidentified samples collected for clinical testing at the Brigham & Women's Hospital (BWH) were provided by the Crimson Core at BWH. No clinical characteristics were available for that cohort. For the cohort of rejection, see Supplementary Tables 1 and 2 for details.
Recruitment	The study was approved by the Institutional Review Board at Brigham and Women's Hospital (2017P000298), and the procedures followed were in accordance with institutional guidelines. For the rejection and BK nephropathy samples, patients were recruited prior to a kidney-transplant biopsy to investigate an elevation of creatinine at BWH. Prospective sample collection was also performed in few kidney-transplant recipients starting in January 2019 and until June 2019. Samples started to be collected one month after transplantation to avoid the impact of surgery and ischaemic time. Samples were then collected according to clinical visits for 3–5 collections within the first year of transplant. The kidney-transplant cohort is representative of kidney-transplant recipients in this geographical location and at a tertiary academic hospital.
Ethics oversight	The research protocol was approved by the Partners Human Research Committee (2017P000298/PHS).

Note that full information on the approval of the study protocol must also be provided in the manuscript.

Clinical data

Policy information about clinical studies

All manuscripts should comply with the ICMJE guidelines for publication of clinical research and a completed CONSORT checklist must be included with all submissions.

Clinical trial registration	Not applicable.
Study protocol	Not applicable. This was not an interventional or randomized trial.
Data collection	Data from transplant recipients were collected from electronic medical records from October 2018 to August 2019.
Outcomes	Outcomes were determined according to kidney-biopsy reports (extracted from electronic medical records) and clinical results of viral copies of BK and CMV (provided by the Crimson Core Lab at BWH).